Proceedings of the XVII ECSMGE-2019
Geotechnical Engineering foundation of the future
ISBN 978-9935-9436-1-3

doi: 10.32075/17ECSMGE-2019-0520

XVII European Conference
ECSMGE 2019
Reykjavik
on Soil Mechanics
and Geotechnical Engineering

Numerical Analysis of an Unsymmetrical Railcar Unloading Pit and Connection Trench

ANALYSE NUMERIQUE D'UN PUITS NON SYMETRIQUE POUR L'EXTRACTION ET LA STOCKAGE DES MINERAUX

C. Fartaria
JETsj, Geotecnia Lda, Lisbon, Portugal
G. Pisco & R. Tomásio
JETsj, Geotecnia Lda, Lisbon, Portugal

J.Costa & J.Azevedo
TECNASOL, Fundações e Geotecnia, Lisbon, Portugal

ABSTRACT: A numerical analysis was performed simulating the deep excavation and dewatering effects on retaining walls of an unsymmetrical railcar unloading pit and trench. The pit has a depth of 22 meters and an internal diameter of 45 meters. The trench is non-collinear with the pit center and it has 12 m width by 122 m length. A 3D Finite Element Model using PLAXIS software was conducted in order to better estimate both general and local effects in the design of the pit's structural elements, mainly due to the singularities introduced by the trench opening on the west side of the pit wall, as well as the trench excavation. Both geotechnical and hydrogeological characteristics of the site were taken into consideration, as well as the main construction stages, covering the excavation sequence and the groundwater inflow analysis.

RÉSUMÉ: Dans cet article ont présent une analyse numérique qui a été développe pour simuler une excavation profonde et l'effet du rebattement de la nappe phréatique dans les murs de soutènement d'un puit non symétrique pour l'extraction et le stockage des minéraux avec l'aide des wagons. Avec une profondeur de 22m et un diamètre intérieur de 45m, le puit circulaire a une intersection de 12m avec une zone en couloir rectangulaire d'accès au puit, placée de façon non aligné avec le centre du puit. Un modelé 3D a été développe avec l'aide du software PLAXIS tenant l'objective d'estimer numériquement les effets locaux e globaux dans le dimensionnent des éléments structurels du puit, en particulier les effets de l´excavation dans la zone d'ouverture correspondent à l'intersection avec le couloir d'accès. Les caractéristiques géotechniques e hydrogéologiques ont été considérés dans le modèle numérique, bien aussi comme les phases des excavations plus importants et l´analyse de l´entrée de l'eau à l'intérieur du puit.
Keywords: deep excavation; 3D finite element model; soil-structure interaction.

1 INTRODUCTION

Deep excavations often comprise a very complex soil-structure interaction. A diversity of aspects must be assessed in order to achieve a safe design, such as geometry, construction sequences, water flow and stress/deformation states. In common practice, 2D plane strain or axisymmetric finite elements models are widely used to analyse geotechnical structures.

However, usually due to geometric singularities, some structures require a three-dimensional analysis in order to ascertain a more accurate global and local soil-structure interaction (Hou et

al. 2009). In this paper it is presented and discussed the numerical analysis of a circular pit deep excavation connected to a non-collinear trench, using both 2D and 3D finite element models.

2 SITE CONDITIONS AND STRUCTURE DESCRIPTION

2.1 Geological and hydrogeological conditions

An extensive site investigation campaign was carried out in order to assess the ground stratigraphic profiling and evaluate the geomechanical and hydrogeological materials' properties. The results of the campaign showed the existence of a superficial alluvium unit, of about 7.5m thickness. Underneath that formation, was observed a sequence of silty clayey material with increasing stiffness up to 29 m depth. Between the silty clay materials and the bedrock formation, a sandy layer was discovered with a thickness ranging from 4 to 12 m. Ordovician bedrock was at 40 m depth , mainly composed by very stiff to hard dark grey to black claystone.

The interpretation of the sand layer behavior was fundamental to the structure's design due to its high permeability when compared with the remaining formations. The upper alluvium and lower clayey layers were characterized by permeabilities of 10^{-6}m/s, while the sandy layer permeability was evaluated as 10^{-5} m/s. Being the sandy layer confined between low permeable soil layers, the water in it is subjected to positive pressures which could affect the stability of the base of the excavation by heave effect (Ou 2006).

Water level measurements were assessed continuously indicating a ground water table level ranging between 1 to 6 m depth. This value is related to ocean ties.

2.2 Retaining wall structures

The structure is part of an industrial complex for aluminum ore extraction and distribution, formed by a main railcar unloading pit and the conveyor system trench. The pit has a circular shape with a diameter of 44.5 with an approximate maximum depth of 22 m. A 12 m width trench is connected from the bottom of the pit to the surface level, over a length of 122 m. Due to site geological, geotechnical and hydrogeological conditions, particularly the position of the phreatic level, a 1 m thick diaphragm wall was designed allowing the excavation of both pit and trench. An isometric representation of the retaining structure is illustrated in Figure 1.

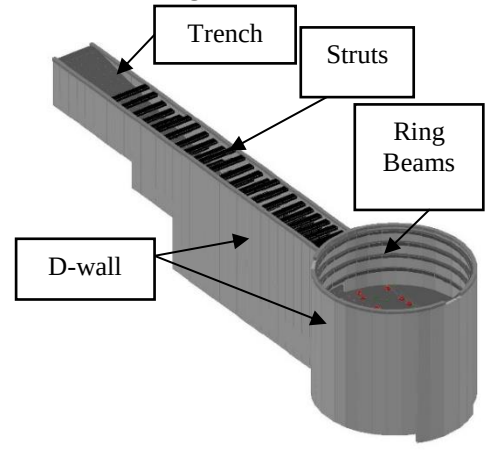

Figure 1. Pit and trench retaining wall isometric view.

An approximately circular pit was shaped with the design of consecutive rectangular D-Wall panels. In order to ensure the D-Wall panels' behave as a continuous structure and also to increase the radial stiffness of the retaining structure, five horizontal levels of reinforced concrete rings were designed (Fig. 2). The fifth ring, placed below the mat foundation level, provided positive support of the D-Wall panels and carry circumferential compression induced by the trench opening. As an additional security measure to prevent eventual lateral water flow through the retaining structure, 800 mm diameter

jet-grouting columns, at the backside of each panel joint, were executed.

In order to avoid lateral instability of the pit's D-Wall panels, on the trench side, four bracing slabs were executed in the backside of those to ensure the transfer of the outward thrust to the trench's D-walls. The horizontal equilibrium of the trench retaining structure was assured by a set of concrete struts (Fig. 3).

In order to avoid hydraulic failure of the low permeable silty clay layers during the excavation works, 7 pressure relief vertical drillings were executed inside the pit and the trench. This drills intersect the sandy layers located beneath the silty clay materials, relieving the hydrostatic pressure of the confined aquifer. To minimize the water flow towards the excavation, the D-Wall panels were design with an average depth of 45 m, assuring a 3 m embedment in the low permeability Ordovician formation.

To ensure the proper foundation of the future structures and to prevent water inflow in the permanent stage, a mat foundation was designed comprising both the pit and the trench. This assures the vertical equilibrium of the long term water pressure that will settle in the bottom of the mat element, with a set of self-drilling micropiles.

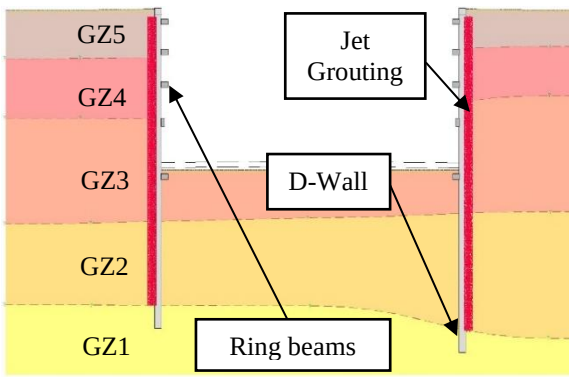

Figure 2. Pit retaining wall cross section.

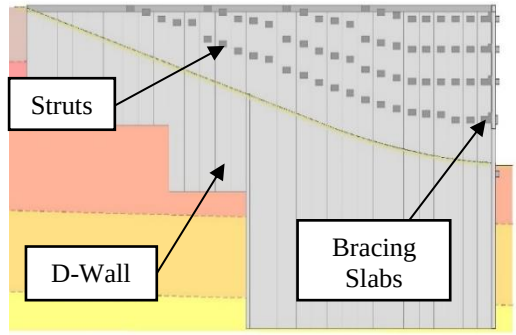

Figure 3. Trench retaining wall longitudinal cross section.

3 NUMERICAL MODELS

3.1 General information

A series of 2D and 3D analyses were carried out using the finite element model program PLAXIS. As a first approach 2D models were developed and later used to validate the 3D global model results and to design the sections that were not under the influence of the pit/trench connection.

The soil behavior was simulated with the Hardening-Soil model (Brinkgreve et al. 2017), an elastic-plastic model with a multi-surface yield criterion that simulate the increase of the soil's stiffness and it's deformation. The following tables (Tab. 1 and Tab. 2) summarize the main parameters that control the behavior of the soil formations. Due to the type of structure and execution technology, it was considered a soil-structure interaction angle 2/3 of soil friction angle, for all the soil layers.

Table 1 – Soil layers and permeability properties.

	M	ms^{-1}
GZ5 -Alluvium	0-7.5	$3.36x10^{-6}$
GZ4 - Silty clay 1	7.5-15.5	$1x10^{-4}$
GZ3 - Silty clay 2	15.5-29.0	$2.1x10^{-10}$
GZ2 - Medium sand	29.0 – 41.0	$1.6x10^{-5}$
GZ1 – Claystone	>41.0	$5.56x10^{-7}$

Table 2 – Soil geomechanical parameters.

Soil	γ_{sat}	c'	φ'	E_{50}^{ref}	E_{oed}^{ref}	E_{ur}^{ref}	m
Layers	kN/m³	kPa	°	MPa	MPa	MPa	-
GZ5	17	3	21	6	6	18	0.8
GZ4	22	8	34	30	30	90	0.8
GZ3	20	35	25	20	20	60	0.8
GZ2	21	0	38	100	100	300	0.5
GZ1	22	40	38	150	150	450	1.0

Despite the low-permeability layers, in typical excavation works, the critical condition is the long-term behaviour of the soils. Therefore, a drained analysis was performed for both excavation and permanent stages in a conservative design option.

Within each model a hydrostatic analysis was conducted considering the water level one meter below the soil surface. The water level variation and hydrostatic pressures were studied according the staged construction sequence and the relief vertical drilling. Additionally, flow analyses were performed on 2D models in order to determine the water flow at the bottom of the excavation and estimate the surface settlements beyond the wall.

3.2 2D retaining wall models

As a first approach, a 2D axisymmetric analysis of the pit's retaining wall was performed, using plate elements with the D-wall's equivalent flexural stiffness, and fixed-end-anchors with the equivalent flexural stiffness of the ring beams. The 2D axisymmetric model mesh is illustrated in Figure 4.

The opening and the trench effect were not included in this analysis, since the axisymmetric analysis simulates a perfectly circular excavation. Another drawback of this model is the impossibility of evaluate the level of the hoop forces on the wall, which have a main role in circular structures that mobilize the arch effect.

Apart from the mentioned limitations, this model represented an important tool in the validation and calibration of a global 3D model. The results of the 2D model were compared with the 3D results. In the elements far from the opening, where its influence is less relevant, an identical soil-structure behaviour was observed.

Due to the longitudinal dimension of the structure, a set of 2D plain-strain models were used were used in the design of the majority of trench's D-wall panels. With the global 3D analysis, it was possible to determine the influence of the opening and, consequently, the range of the 2D analysis. As in the previous case, the trench's 2D plain-strain models were used in the 3D model validation.

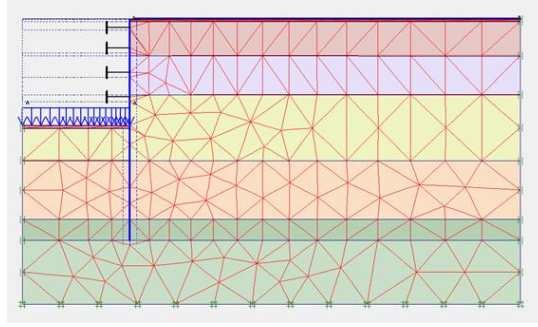

Figure 4 – 2D Axisymmetric pit retaining wall model - mesh.

3.3 3D Global retaining wall model

3.3.1 Model definition

Since, both general and local effects in the structural design of the pit and trench were not possible to model with 2D models, it was developed a 3D global finite element model. Figure 5 illustrates the 3D global model mesh.

With a geometry of 200 m x 150 m and 66.5 m depth, the 3D model mesh has 137692 finite elements and 2065380 nodes. The mesh density was optimized using local coarseness features. To reduce the model size and to avoid numerical errors some simplifications were taken into consideration. Therefore, the trench length was reduced and the excavation depth was constant.

The D-Wall panels for both pit and trench retaining walls and bracing slabs were modelled

through plate elements with equivalent flexural stiffness. Considering that the constructive technology of D-walls imposes a non-monolithic connection between successive panels, a hinged connection was modelled between plate elements. The capping beams, the trench concrete struts and the pit ring beams were modelled with beam elements with equivalent stiffness. Tables 3 and 4 summarize the plate and beam element properties.

Table 3 – Plate elements properties.

Structural	d	ϒ	E	ν_{12}	G_{12}
Element	m	kN/m^3	MPa	-	MPa
D-Wall	1.0	25	34	0.2	14.17
Bracing Slab	0.85	25	34	0.2	14.17

Table 4 – Beam elements properties.

Structural	A	ϒ	E	I_3	I_2
Element	m^2	kN/m^3	MPa	m^4	m^4
Struts (200x85mm)	1.7	25	34	0.102	0.567
Ring 4 (100x80mm)	0.8	25	34	0.043	0.067
Rings 1,2,3 and 5 (50x120mm)	0.6	25	34	0.072	0.013
Capping beam (1000x1000mm)	1.0	25	34	0.083	0.083

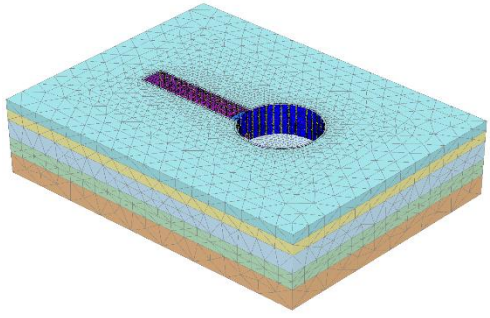

Figure 5 – 3D Global model isometric view – plate elements.

3.3.2 Model singularities

The main aspects captured with the 3D model were the local and overall behaviour introduced by the trench excavation on the west side of the pit as well as, in a later stage, the trench/pit opening. The resultant imbalance in the back of the pit's retaining walls was accounted and balanced with bracing slabs elements. The relative orientation of the trench to the pit was another important issue, since they were not concentric. In the 3D model, the D-wall panels were defined by plate elements with the executed dimensions and were consecutively disposed in order to simulate the real geometrical conditions of the pit retaining wall.

The 3D global model allowed the modelling of the T-panels that connect the trench and pit's structure. For constructive reasons, the web and the flange cage were placed disjointedly so both translational and rotational degrees of freedom were released in those connections. Figure 6 illustrates the model at the zone of the pit/trench

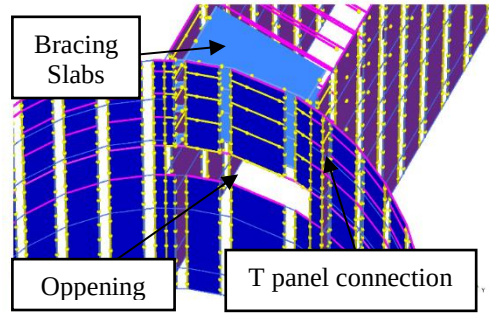

Figure 6 – 3D global model view of the trench/pit connection.

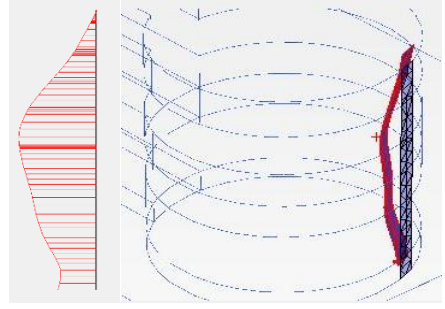

Figure 7 – Pit retaining wall vertical bending moment diagram: 2D axisymmetric model [maximum value: 272 kNm/m] (left) and 3D global model [maximum value: 345 kNm/m] (right).

interception. It can be observed the visible opening, pinned connections between panels and bracing slabs.

4 NUMERICAL MODEL RESULTS

4.1 2D vs. 3D Pit retaining wall model results.

An analysis comparing the results of the pit's retaining wall stresses and deformations on both the 2D axisymmetric and 3D global models was established, particularly at the opposite side of the pit where its influence was expected to be minor. The main results of the two models, for that section concerning the final excavation stage, are illustrated in the figures 7, 8 and 9.

Regarding the retaining wall bending moments, the results obtained in both models (Fig. 7) show a reasonable approximation concerning diagrams and maximum values reached. Bending moments diagrams are very similar, the peak values for both positive and negative moments are well defined and located at approximately the same depths in both models, showing a value difference of about 20%.

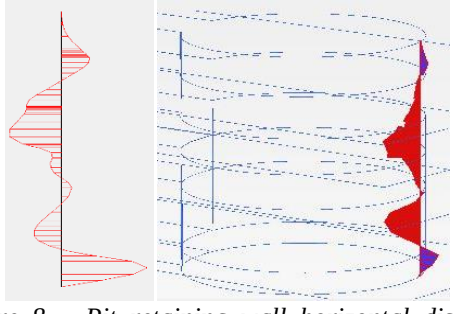

Figure 8 – Pit retaining wall horizontal displacements: 2D axisymmetric model [maximum value: 5 mm] (left) and 3D global model [maximum value: 6 mm] (right).

The horizontal displacement diagram reveals similarities between the two models, and the estimated maximum displacement values are almost identical (Fig. 8).

For a preliminary calculation of the hoop forces, was taken into consideration the effect of earth pressure, ground water pressure and surcharges. In order to simplify the calculation, the stresses were calculated at the depth were higher hoop forces were expected and for an equivalent soil layer with average geomechanical parameters of all soil layers. With a radius of 22,25 m and an estimated load of 365 kPa, a maximum hoop stress of 8121 kN/m was predicted.

Regarding the normal stress in the tangential direction, referred as hoop forces, although values obtained in 2D model were higher than the 3D model ones, their magnitude is similar and within the order of magnitude predicted by the simplified calculation (Fig. 9). The diagrams agree in both models and, as expected, the hoop forces increase with depth.

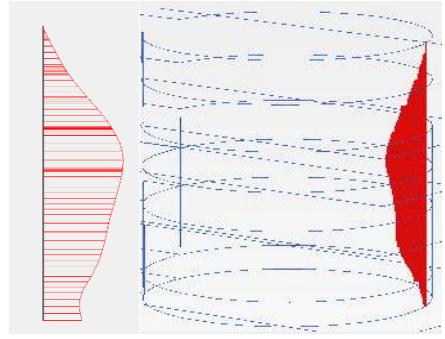

Figure 9 – Pit retaining wall hoop forces diagram: 2D axisymmetric model [maximum value: 7864 kN/m] (left) and 3D global model [maximum value: 6270 kN/m] (right).

4.2 2D vs. 3D Trench retaining model results

In order to study the oppening effect in the trench wall's behaviour, the 2D model results were compared with the 3D model near the mention area. The trench retaining wall stresses and deformations were analysed.

The main results of the two models, for that section and concerning the final excavation stage, are illustrated in the figure 10 to 12. Regarding the 2D model results, it was observed a typical behvior of a retaining wall with multiple passive horizontal supports (Fig. 10).

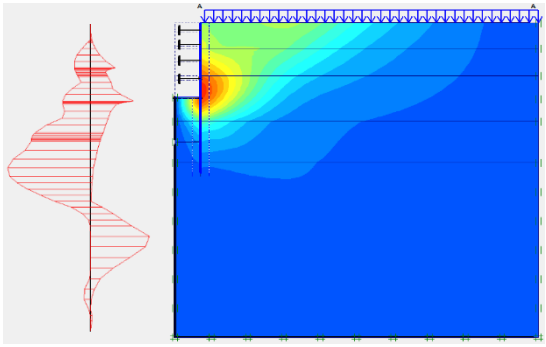

Figure 10 – Trench retaining wall horizontal displacements: 2D plane strain model [maximum value: 41 mm] (left); and bending moment diagram [2381 kNm/m] (right).

Results from the 3D model at a section with the same horizontal supports and excavation depth showed identical deformations and stresses (Figs. 11 and 12), despite the expected difference.

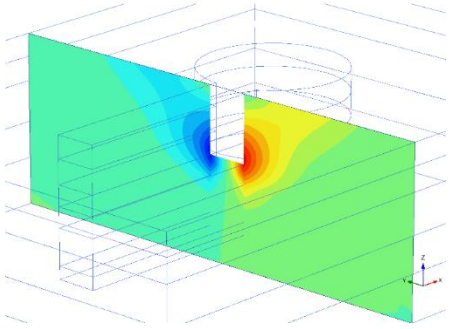

Figure 11 – Trench retaining wall horizontal displacements: 3D global model [maximum value: 35mm].

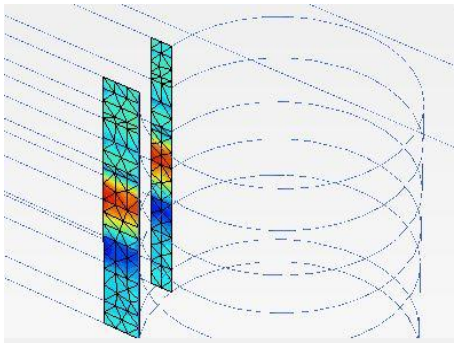

Figure 12 – Trench retaining wall vertical bending moment diagram: 3D global model [maximum value: 2552 kNm/m].

From the previous assessment, it is possible to conclude that the ring beams and bracing slab elements guaranty the overall stability of the pit walls and have a lower impact in trench retaining walls.

4.3 3G Global retaining wall model results

Although the 3D global model was developed aiming mainly to validate previous models and simplified calculations, as well as to determine the overall behaviour of the retaining structure, it was also essential in the design of local singularities. The trench/pit connection opening was modelled at the final stage and its effect was observed within the near elements (Fig. 13).

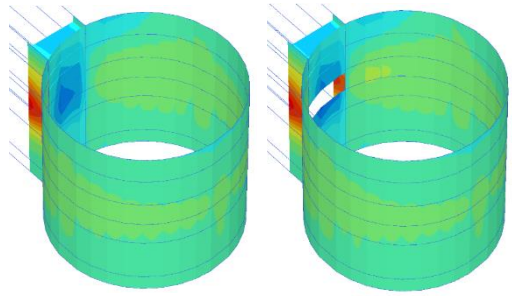

Figure 13 – Retaining wall horizontal displacements: 3D model before (left) and after the opening (right).

The design of the structural elements affected by the opening was validated with simplified calculations, particularly the nearest ring beams, where an increase in its axial forces was expected and had to be assessed (Fig. 14).

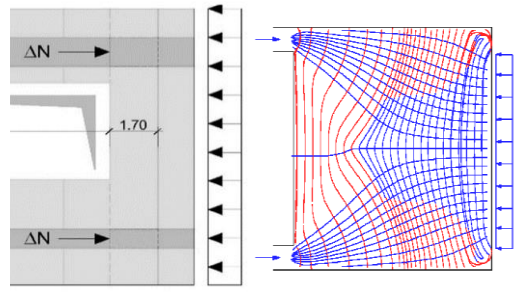

Figure 14 – Simplified model for hoop forces increase due to opening (left). Expected stress path due to opening (right).

The 3D model was also fundamental to obtain the bracing slabs' stresses, since they transfer the outward thrust to the trench retaining walls, resolving the imbalance caused by the trench excavation. The model results confirm the vital role of this elements in the overall stability of the retaining walls. Regarding the walls, due to relevant axial loads in both plan directions, a combined bending axial forces interaction was used at the reinforcement design. Also, the absolute value of torsional bending has been totally added to flexural bending moments on both directions. Absolut values of vertical and horizontal shear has been totally added, considering a total shear acting out of plane. The bracing slab/d-wall interface connection was also design based on the model results. The effect caused by the opening was also observed on the bracing slabs elements, confirming the 3D global model importance since the trench/pit connection opening led to a significant increase of the axial load of the bracing elements, approximately 40% (Fig. 15).

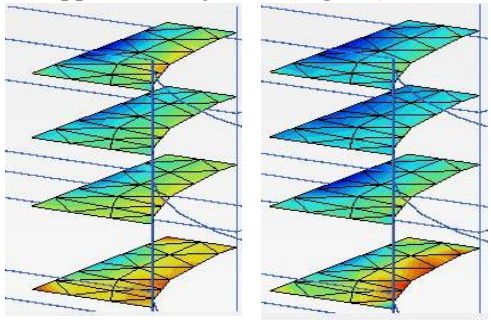

Figure 15 – Bracing slabs axial forces N2 before [maximum value: 3665 kNm/m] (left) and after the opening [maximum value: 5232 kNm/m] (right).

5 FINAL REMARKS

Finite element analyses have been carried with both 2D and 3D models in order to simulate a deep excavation and the necessary dewatering effects for the execution of an unsymmetrical railcar unloading pit and its connection trench. As a first approach, 2D analyses were performed for both pit and trench retaining wall modelling. Those analyses covered separately the pit, exploiting its cylindrical symmetry to establish an axisymmetric model, and the trench, due to its overall length modelled within a plane strain analysis.

Due to the noncollinearity between the trench alignment and the pit center, the overall stability and behaviour of the structure needed to be assessed. The connection between structures was studied in detail with the aim of understanding their influence on the different elements of the structure. A 3D global model was developed in order to study all the singularities, being validated and calibrated with 2D numerical analyses. The numerical analyses' results, from the 2D and 3D models, showed, in generally, a good agreement, in the areas far from the singularities. Some conclusions on the validity of the 2D models within some parts of the structure were taken and used in the elements design. The 3D model was particularly useful on the analysis of some structural elements, allowing a better understanding of the overall behaviour. Concerning the flow analysis, the 2D models revealed to be adequate.

Since 3D calculation can be time consuming, 2D prelaminar analyses can be performed, even when a 3D analyses is geometrically crucial, enabling some initial design calculations and consequentially increasing the level of development of the structure conception for a subsequent implementation in a 3D model. Rather than opposites, 2D and 3D calculations showed to be useful complementary tolls in the design of complex tridimensional structures.

The instrumentation readings validate the model results, showing a good agreement between the measurements and simulated values, both in terms of displacements and water inflow.

6 REFERENCES

Brinkgreve, R.B.J. & Kumarswamy, S. & Swolfs, W.M. 2017. *Plaxis – Material Models Manual 2017*, Delft: Plaxis bv

Hou,Y.M. & Wang, J.H. & Zhang, L.L. 2009. Finite-element modeling of a complex deep excavation in Shanghai. *Acta Geotechnica* 4:7-16. Shanghai, China

Ou, C.Y. 2006. *Deep Excavation – Theory and Practice*. London: Taylor & Francis Group